AD-A086 605 ORINCON CORP LA JOLLA CA F/6 17/1
A CASE STUDY IN ADAPTIVE SOUND SPEED ESTIMATION,(U)
1978 R N LOBBIA, D L ALSPACH N00014-77-C-0296
UNCLASSIFIED NL

END
DATE FILMED
8-80
DTIC

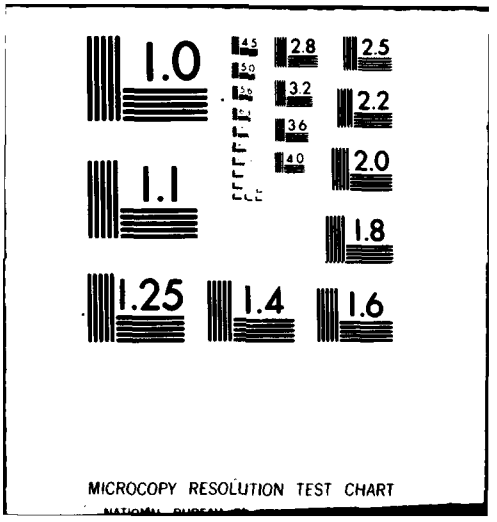
1.0
1.1
1.25
1.4
1.6
1.8
2.0
2.2
2.5
2.8
3.2
3.6
4.0
MICROCOPY RESOLUTION TEST CHART

4. "A Case Study in Adaptive Sound Speed Estimation," by R. N. Lobbia and D. L. Alspach, was presented at and appears in the Proceedings of the November 1978 Asilomar Conference on Systems Science.

DOCUMENT 4

A CASE STUDY IN ADAPTIVE SOUND SPEED ESTIMATION

ORINCON

A CASE STUDY IN ADAPTIVE SOUND SPEED ESTIMATION

by

(10) R. N. Lobbia D. L. Alspach

ORINCON Corporation
3366 N. Torrey Pines Ct., Suite 320
La Jolla, CA 92037

ABSTRACT

This paper deals with the problem of sound speed estimation as an aid in improving our knowledge of the position of a drifting sonobuoy. This is accomplished by processing the outputs of a spatially displaced set of hydrophone sensors in an extended Kalman filter. The filter's state vector may be augmented to provide estimates of the sonobuoy's position, velocity, and the sound speed from the sonobuoy to each of the hydrophones.

It is shown that with just time-of-arrival difference and doppler difference measurements, system observability is marginal – directly resulting in biased estimates of the sonobuoy's location. With the additional use of bearing measurements, it is then shown how this enhances system observability and, consequently, estimation performance.

1. INTRODUCTION

In this paper, we are concerned with the accurate location of a sonobuoy over a specified interval of time. It is assumed to be subjected to both random and deterministic forces over this same time period. Because of this, our knowledge of the sonobuoy's location is uncertain and can be in error if we employ conventional dead reckoning methods.

Another approach more accurate than the above would be to place a source emitting a continuous pseudorandom gaussian signal aboard the sonobuoy. A set of three or more passive hydrophones, geographically separated from one another, can then be used to pick up the sonobuoy's signal to provide measurements of sound time-of-arrival difference and doppler difference. As an example, one configuration involving three hydrophones is shown below in Figure 1.

In this figure R_i, $i=1, 2, 3$ represents the distance from the sonobuoy to each of the hydrophones and c_i, $i=1, 2, 3$ represents the sound speed to each hydrophone. Note that we are using three distinct sound speeds instead of a single one. This is because sound speed, in a thermally non-homogeneous medium, is related in a complex fashion to such variables as time-of-day, distance between hydrophone and sonobuoy, bearing of hydrophone with respect to sonobuoy, etc.

Now if we consider any pair of hydrophones, pair 1-2 for instance, then we can obtain, through cross-correlation methods, two measurements, time-of-arrival differences and doppler difference, that are related to the sonobuoy's location by the following equations:

$$\tau_{1\text{-}2} = \frac{R_1}{c_1} - \frac{R_2}{c_2} \tag{1}$$

$$\alpha_{1\text{-}2} = \frac{\dot{R}_1}{c_1} - \frac{\dot{R}_2}{c_2} \tag{2}$$

In Equation (1), $\tau_{1\text{-}2}$ represents the sound time-of-arrival difference for the hydrophone array pair 1-2. $\tau_{1\text{-}2}$ in Equation (2) represents the normalized doppler difference, $\frac{\Delta f}{f}$, where f is the base frequency of the narrowband source.

Using spherical geometry, the distances R_i and time rate-of-change distances $\dot{R}_i$ are related to the sonobuoy's location by the following equations:

$$R_i = \cos^{-1}\left[\sin x_1 \sin\lambda_i + \cos x_1 \cos\lambda_i \cos(x_2 - \theta_i)\right] \tag{3}$$

$$\dot{R}_i = \frac{x_3\left[\sin x_1 \cos\lambda_i \cos(x_2 - \theta_i) - \cos x_1 \sin\lambda_i\right]}{\sin R_i} + \frac{x_4 \cos x_1 \cos\lambda_i \sin(x_2 - \theta_i)}{\sin R_i} \tag{4}$$

where

x_i, $i=1, 2, 3, 4$ represents the sonobuoy latitude, longitude, latitude rate, and longitude rate, respectively.

λ_i, θ_i represents the latitude and longitude of the i^{th} hydrophone.

In Equation (4) it was assumed that each of the hydrophones was stationary.

Because of the nonlinear feature of the above measurement equations, it is very difficult to solve explicitly for the sonobuoy's state vector (x_1, x_2, x_3, x_4). In the next section, it will be shown how this state vector may be obtained in a recursive manner using an extended Kalman filter.

Following this we will show that when the sound speeds are imprecisely known, then estimates of the sonobuoy's position and velocity become biased. Section 3 then presents a method for augmenting the sound speeds to the sonobuoy state estimate and it is shown that the augmented state becomes marginally observable. This directly results in biased estimates for the sonobuoy's state vector. We then show that the additional use of bearing measurements are seen to enhance system observability to the point where estimation of the sonobuoy state vector becomes unbiased.

Finally, in Section 4, we will summarize our results.

2. ESTIMATION OF SONOBUOY STATE VECTOR

It is apparent from Equations (1) to (4) that it would be difficult to solve for the sonobuoy state vector in terms of the measurement $\tau_{i,j}$, $\alpha_{i,j}$. A recursive approach may be sought that avoids this difficulty. The approach we use here involves application of an extended Kalman filter.

In order to implement this filter, we need in addition to the measurement Equations (1) to (4), a model for the dynamics of the system. This is easily obtained when we assume a constant speed and constant course drift and, in addition, a random perturbation to account for modeling uncertainties, environmental forces, etc. In discrete-time form, the equations for the system dynamics are given by:

$$\underline{x}(k+1) = \underbrace{\begin{bmatrix} 1 & 0 & \Delta t & 0 \\ 0 & 1 & 0 & \Delta t \\ 0 & 0 & 1 & 0 \\ 0 & 0 & 0 & 1 \end{bmatrix}}_{\Phi(\Delta t)} \underline{x}(k) + \underbrace{\begin{bmatrix} 0 \\ 0 \\ w_3(k) \\ w_4(k) \end{bmatrix}}_{\underline{w}(k)} \qquad (5)$$

where

$$\underline{x}(k) = \begin{bmatrix} x_1(k) \\ x_2(k) \\ x_3(k) \\ x_4(k) \end{bmatrix}$$ is the sonobuoy state vector

Δt = sampling interval

$w_3(k)$, $w_4(k)$ are zero mean, random, white noise sequences

$E\left\{\underline{w}(k)\underline{w}^T(j)\right\} = Q_k \delta_{kj}$; δ_{kj} is the Kroneker Delta.

If we linearize the measurement equation about our most recent estimate of the state, $\hat{x}(k)$, to obtain a linear measurement matrix, $H(\hat{x}(k))$, we can then implement the extended Kalman filter in real time. In vector-matrix form, these equations are recursively given by [3]:

$$\hat{x}(k+1/k) = \Phi(\Delta t)\,\hat{x}(k/k) \qquad (6)$$

$$P(k+1/k) = \Phi(\Delta t)\,P(k/k)\,\Phi^T(\Delta t) + Q_k \qquad (7)$$

$$\hat{x}(k+1/k+1) = \hat{x}(k+1/k) + K_k\left[z_k - h(\hat{x}(k+1/k))\right] \qquad (8)$$

$$P(k+1/k+1) = \left[1 - K_k H(\hat{x}(k+1/k))\right] P(k+1/k) \qquad (9)$$

$$K_k = P(k+1/k)\,H(\hat{x}(k+1/k))\left[H(\hat{x}(k+1/k))\,P(k+1/k)\,H^T(\hat{x}(k+1/k)) + R_k\right]^{-1} \qquad (10)$$

Equations (6) and (7) represent predictions of the state estimate and covariance to time (k+1), whereas Equations (8) through (10) update the state estimate and covariance to account for a new measurement. In the latter set of equations, the measured vector is given by $z_k^T = [\tau_{i,j}(k), \alpha_{i,j}(k)]$, where $h(\cdot)$ represents the nonlinear dependence of z_k on $x(k)$ defined by Equations (1) through (4). R_k is the covariance matrix of an additive white-noise measurement sequence. $H(x(k+1/k))$ is the measurement equation that is linearized about the most current state estimate and is defined by:

$$H(\hat{x}(k+1/k)) = \left.\frac{\partial h(\hat{x}(k))}{\partial \hat{x}(k)}\right|_{\hat{x}(k) = \hat{x}(k+1/k)}$$

This linearization was found to accurately describe the functional characteristics of the nonlinear measurement model as $H(\cdot)$ was relatively insensitive to variation in $\hat{x}(k)$.

These equations were implemented in the case where we knew the sound speeds to each hydrophone. Under these circumstances, the resulting estimation performance was seen to be excellent.

However, for the case involving unknown sound speeds, the estimation performance degrades rapidly when we use incorrect values for the sound speeds in the Kalman filter. An example of this is shown in Figures 2 and 3 for a case involving an average sonobuoy drift velocity of 1 knot and course of 45 degrees. In Figure 2, the solid curves represent motion of the truth model and the dotted curves represent estimates of the sonobuoy state as provided by a Kalman filter. The measurements were assumed noisy with a standard deviation in τ and α of .1 second and 1×10^{-5}, respectively. The estimation error and a priori/a posteriori standard deviations are presented in Figure 3. A set of three hydrophones were configured essentially as vertices of an equilateral triangle with the sonobuoy starting near the center of this triangle. The truth model sound speeds were set at: c_1 = 4857 ft/sec, c_2 = 4957 ft/sec, and c_3 = 4757 ft/sec around nominal values from Urick [1]. The filter used an incorrect value of 5000 ft/sec for all three speeds and no attempt to estimate them was made. It is clear from Figure 2 that significant biases in estimated position and speed develop.

In the next section, we will see how the use of bearing measurements enhances system observability and allows unbiased estimation of the sonobuoy state vector.

3. SOUND SPEED ESTIMATION

Because of the biases that develop when we use incorrect sound speeds in the Kalman filter, it was felt that estimation of these sound speeds in addition to the sonobuoy states would eliminate the biases. This is done simply by augmenting the sound speeds to the original four element sonobuoy state vector. The assumption was made that the sound speed was constant and unknown over a sufficiently long time interval. Its state equation is then given by:

$$\dot{c}_i = 0; \quad i = 1, 2, 3 \qquad (11)$$

Implementation of the extended Kalman filter for the augmented state vector is therefore rather simple and straightforward and will not be presented here.

Upon implementing the augmented state filter, it was found that biases still developed in the sonobuoy states and sound speeds for a number of scenarios involving different starting positions, speeds, courses, etc. For this reason, the observability of the linearized, augmented state system was explored using the information matrix [2]. In the situation involving no process noise and state vector a priori information, the information matrix is equal to the inverse of the Kalman filter covariance

matrix, $P^{-1}(k/k)$. This matrix must be positive definite for stochastic observability and, provided the above conditions apply, is given in recursive form by:

$$P^{-1}(k/k) = \Phi^T(-\Delta t)\, P^{-1}(k-1/k-1)\, \Phi(-\Delta t) + H^T(\bar{x}(k-1))\, R_k^{-1}\, H(\bar{x}(k-1)); P^{-1}(0/0) = 0 \quad (12)$$

where $\Phi(\Delta t)$ is the state transition matrix defined in (5), $H(\bar{x}(k-1))$ is the measurement matrix linearized about the state vector $\bar{x}(k-1)$.

To assess the property of stochastic observability, the normalized eigenvalues of this matrix were computed (normalized to one) and plotted as a function of time. Figure 4 shows the results that were obtained for the case involving one unknown and constant sound speed. One of the sonobuoy position eigenvalues becomes ill-conditioned and exhibits a smaller maximum magnitude than the other position eigenvalue by a few orders of magnitude. This analysis was repeated for a number of different sonobuoy starting positions and headings, and the same general result was obtained, i.e., ill-conditioned behavior of one of the eigenvalues. Because of this and the fact that the state estimates were biased, we concluded that the system was marginally observable.

As a means of improving the property of system observability, we introduced an additional measurement of bearing to use in the Kalman filter. We assumed that it was contaminated by additive white noise with a standard deviation of .1 degree. These measurements defined the bearing of the sonobuoy with respect to each hydrophone, and are normally available as outputs from the same set of hydrophones without introducing additional sensors.

The Kalman filter was then rerun with these additional measurements and the sonobuoy tracking performance was found to be very good. Figures 5, 6, 7, and 8 summarize the results of one case where we estimate the four sonobuoy states and three sound speeds. In Figure 5, convergence of the sonobuoy state estimates to their true values is seen to be very rapid. Noise was introduced in the sound speed truth model to add more realism to the problem and this variation is reflected by the variation in sound speed of the truth model as shown in Figure 6. Figures 7 and 8 present estimation error and standard deviations of the sonobuoy states and sound speeds. These errors are seen to fall well within the ± two-sigma value as one would expect for unbiased estimation. A number of other cases were also run and are not presented here because of space limitations. For these other cases it was found that tracking performance was as good as before and all of the earlier noted biases in the state estimates, when processing only time-delay and doppler difference measurements, had disappeared.

4. CONCLUSIONS

To summarize the above results, we saw that to estimate the sonobuoy position and velocity accurately we need to also estimate the sound speeds to each hydrophone when they are unknown. With the aid of the information matrix we found that the linearized system was marginally observable when attempting to estimate both the sonobuoy states and sound speeds.

Because the linearized measurement model accurately represented its nonlinear counterpart, we concluded that the nonlinear system was also marginally observable. This was also reflected by the biased estimates of sonobuoy position when implementing the Kalman filter.

Finally, by incorporating and additional independent measurement (bearing) the system observability was enhanced considerably and we were then able to track the sonobuoy's motion quite accurately.

Although not reported in the last section, we also looked at the use of time-delay and doppler difference measurements of more than three hydrophones (as opposed to time delay, doppler difference, and bearing measurements of just three hydrophones) as a means of improving system observability. In general, it was found that if one had n hydrophones with n unknown sound speeds from the sonobuoy to each hydrophone, then we could at most estimate the sonobuoy state vector and (n-1) sound speeds; one of these sound speeds had to be known exactly when implementing the Kalman filter.

At the present time, we are continuing research in this area of sonobuoy state and sound speed estimation to more fully explore the sensitivity of the estimation process to geometrical placement of the hydrophones, time between measurements, etc.

ACKNOWLEDGMENTS

The authors wish to express their appreciation to Dr. W. Marsh and Dr. G. Mohnkern of the Naval Ocean Systems Center (NOSC) for their support and helpful suggestions during the course of this research, and to J. Hellmer and J. McRoberts (NOSC) for their assistance in completing the computer analyses in this paper.

REFERENCES

[1] R. J. Urick, *Principles of Underwater Sound for Engineers*, McGraw Hill, 1967

[2] A. H. Jaywinski, *Stochastic Processes and Filtering Theory*, pp 231-234, Academic Press, 1970

[3] J. S. Meditch, *Stochastic Optimal Linear Estimation & Control*, McGraw-Hill, 1969

This work was partially supported by the Office of Naval Research under Contract N00014-77-C-0296

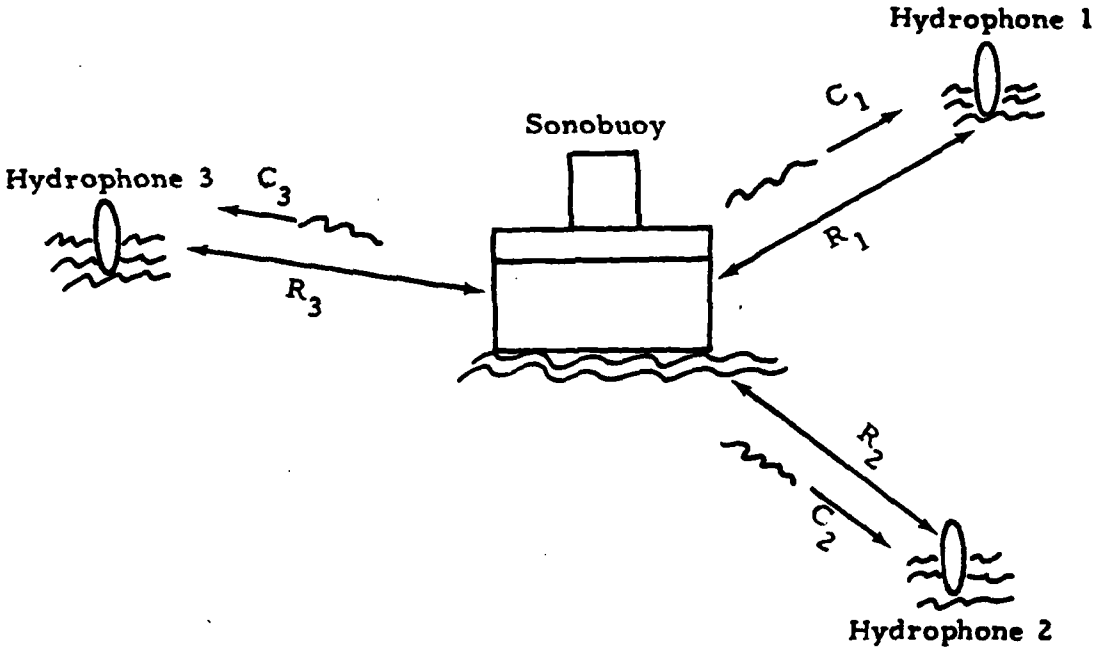

Figure 1. Hydrophone/sonobuoy geometry.

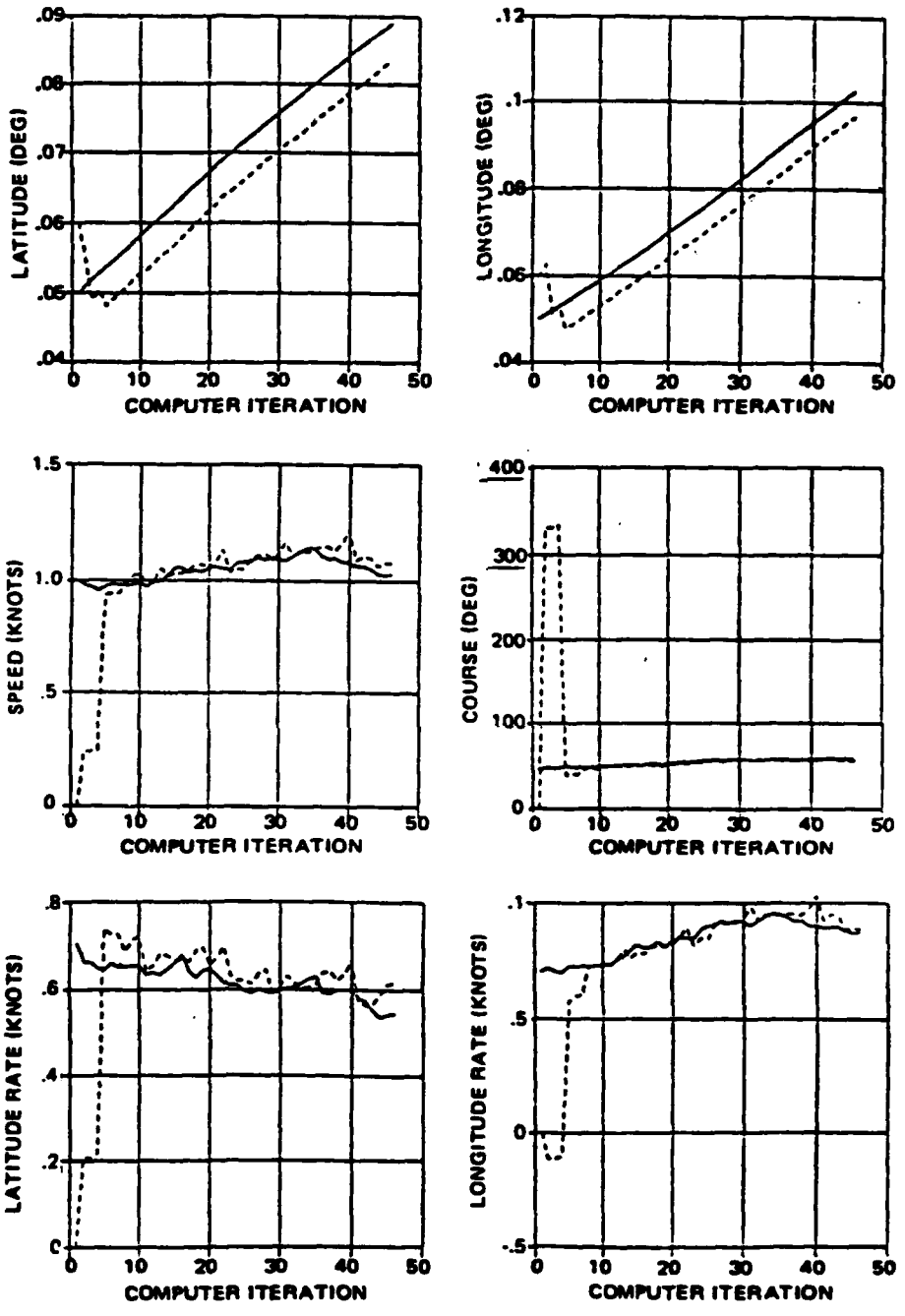

Figure 2. Estimation of sonobuoy states using incorrect sound speeds.

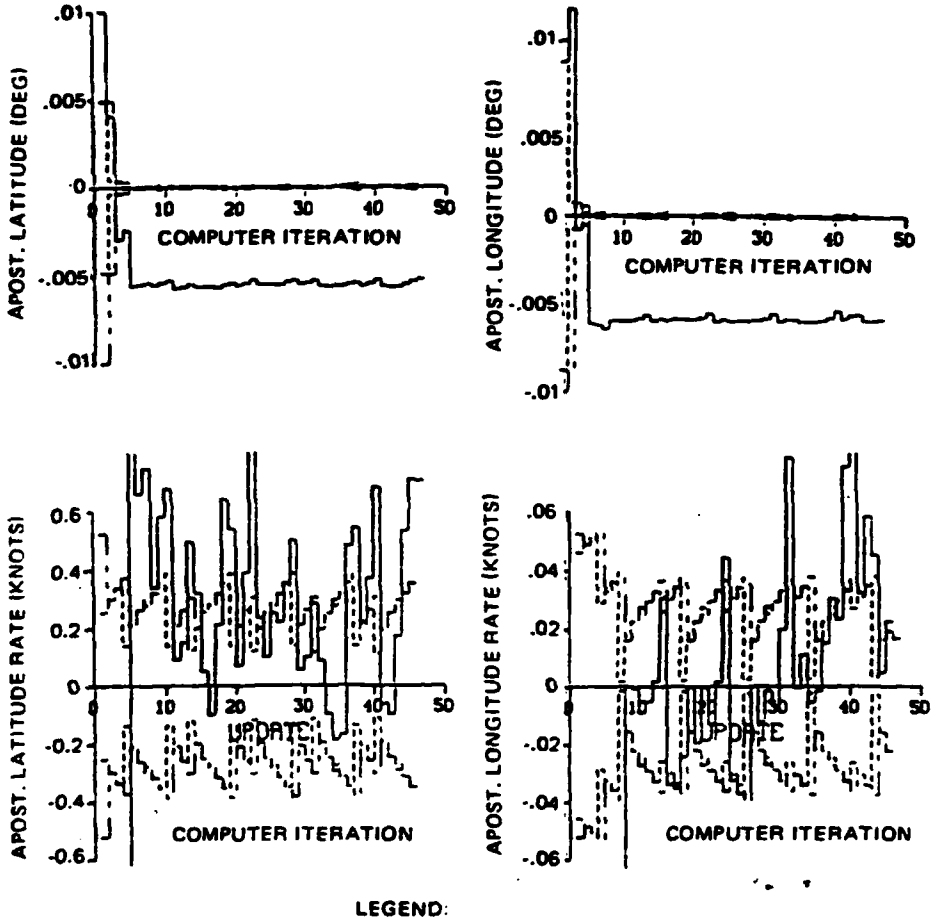

LEGEND:
DASH – APOST. STD. DEV.
SOLID – STATE ERROR
CHNDOT – APRIOR STD. DEV.

Figure 3. Sonobuoy estimation error and standard deviation—incorrect sound speeds.

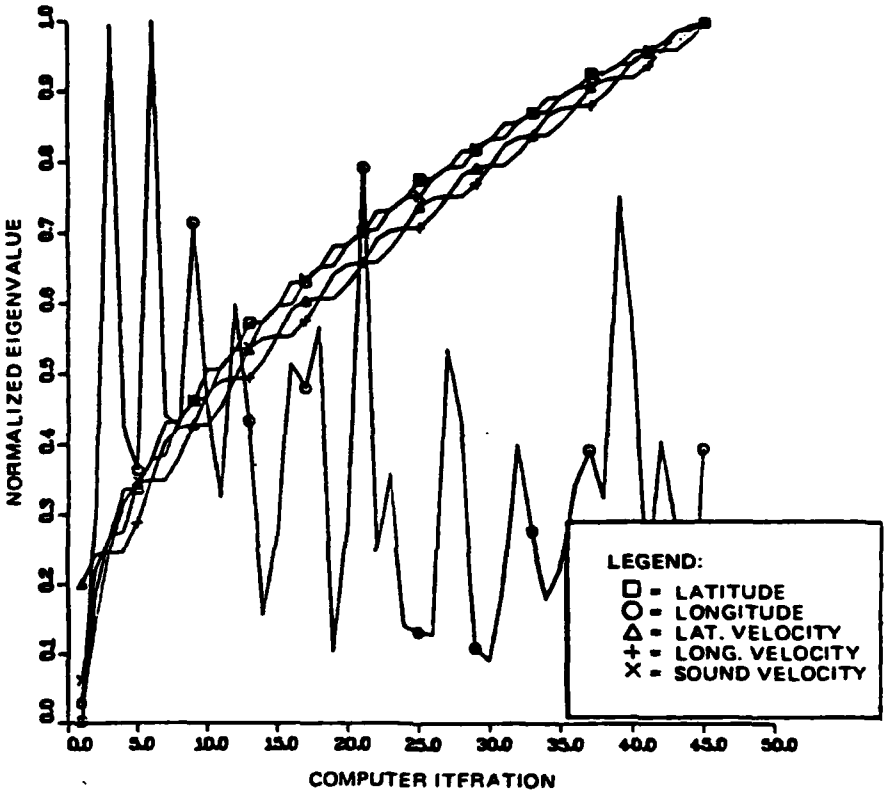

MAX:LAT. = 6.223+02 LONG. = 8.598+00

MAX.LAT. RATE = 3.189+01
:LONG. RATE = 2.767+01

SOUND SPEED = 1.420+00

COURSE = 90

Figure 4. Normalized eigenvalues of the information matrix.

ORINCON

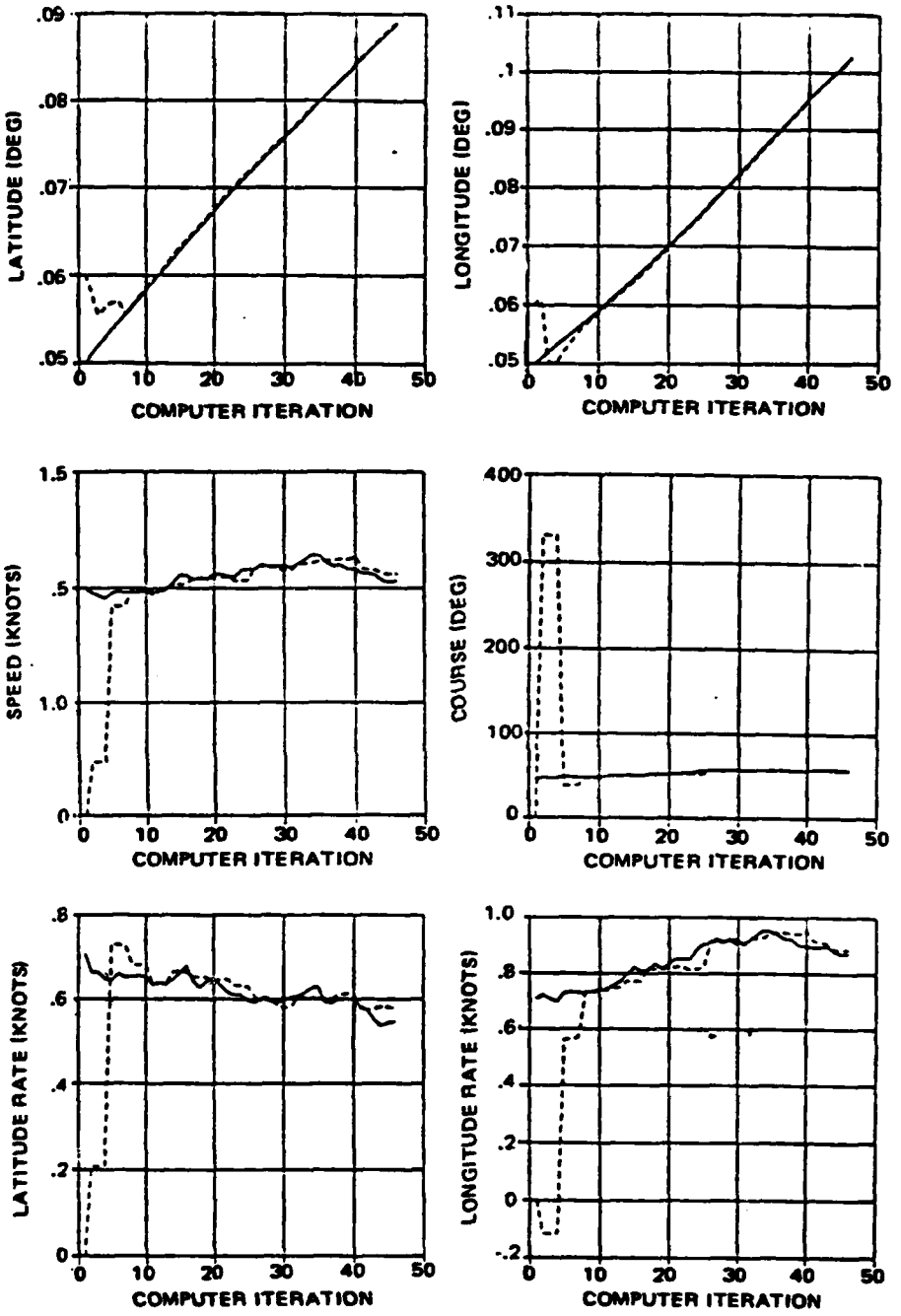

Figure 5. Estimation of sonobuoy states.

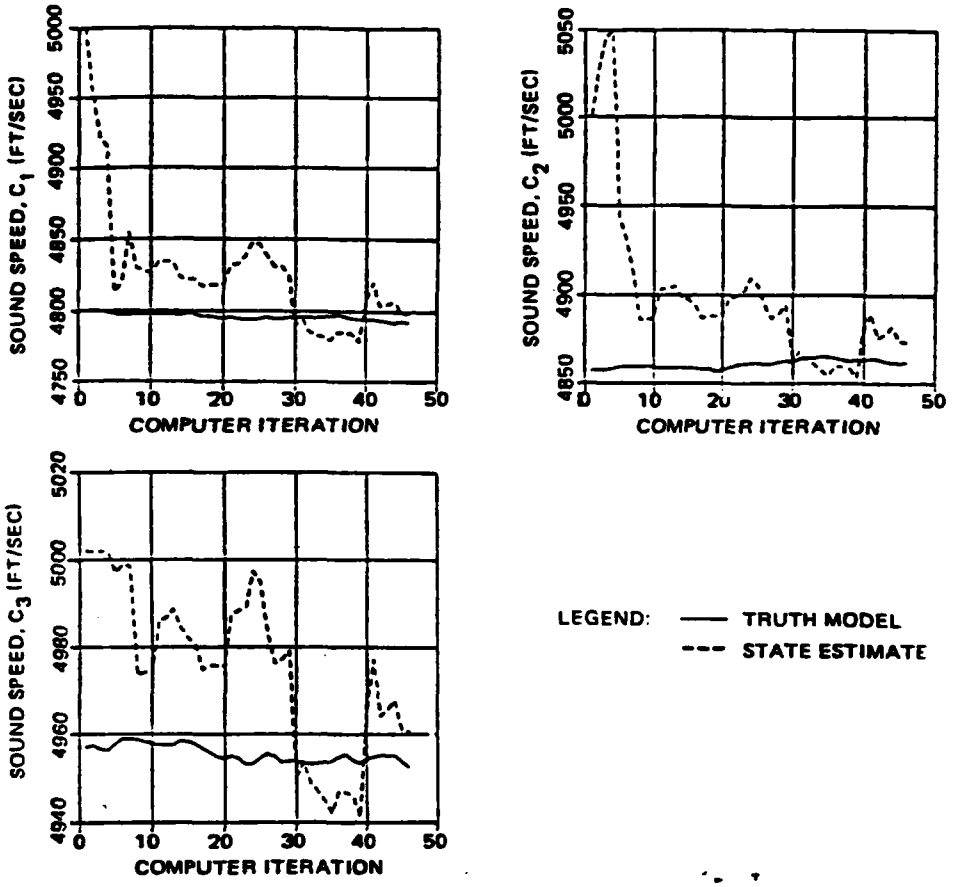

Figure 6. Estimation of sound speeds.

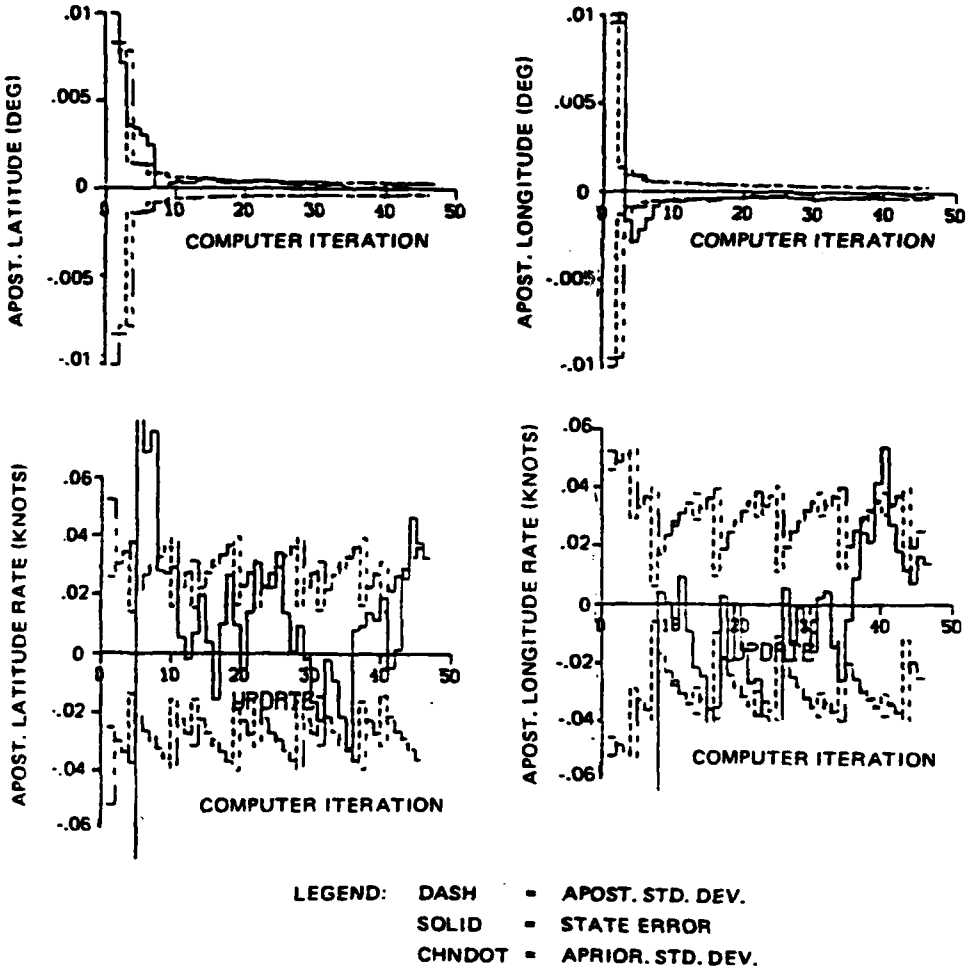

Figure 7. Sonobuoy estimation error and standard deviation.

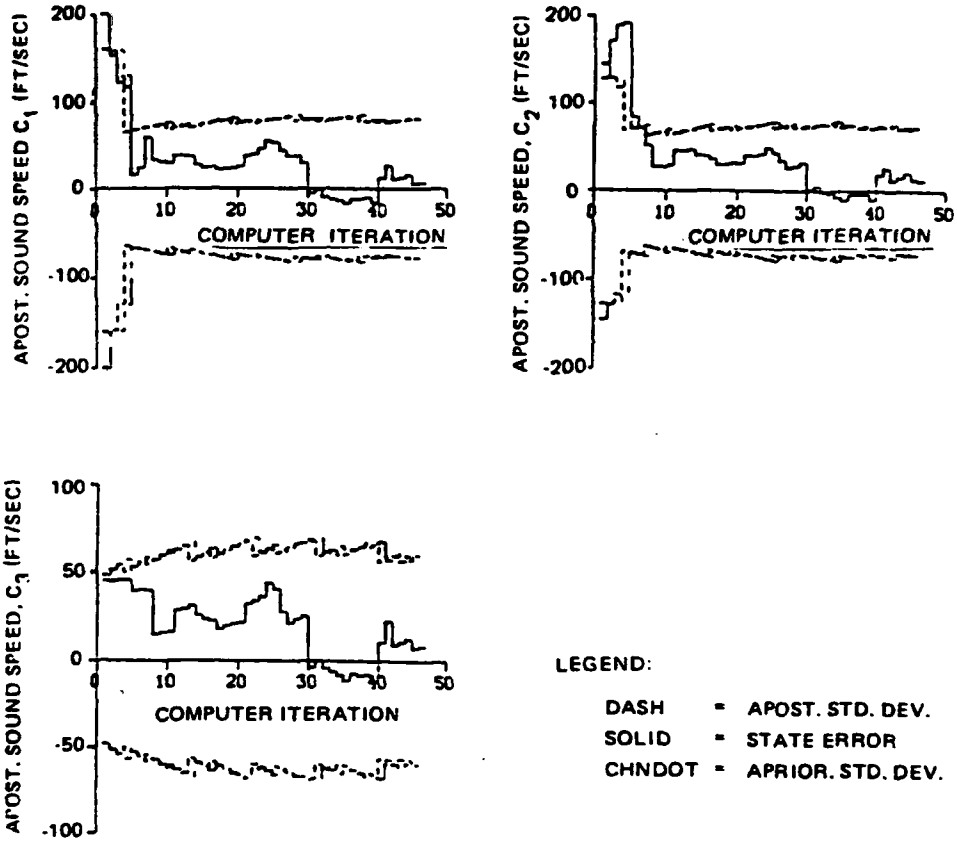

Figure 8. Sound speed estimation and standard deviation.


DAT
FILM